JOURNAL OF MATERIALS SCIENCE 22 (1987) 2332–2340

Electrical conductivity and creep of polycrystalline α-Al_2O_3 doped with titanium or iron plus titanium

J. M. TSAUR, F. A. KROGER
Department of Materials Science, University of Southern California, Los Angeles, California 90089-0241, USA

Creep and conductivity were measured for polycrystalline α-Al_2O_3 doped with titanium or iron plus titanium. Both series of samples show a transition from acceptor domination to donor domination at the point where the concentrations of titanium and acceptors are approximately equal. Parameters in the expression for the creep rate $\dot{\varepsilon} \propto S^n d^{-p} P_{O_2}^r \exp(-Q/kT)$ (where S is the applied stress, d the grain size, Q an activation energy and n, p, r are constants characterizing the creep mechanism) indicate limitation by bulk diffusion in the acceptor-dominated samples and in the donor-dominated samples at low [Ti]. In the latter samples the rate-limiting species is O_i'' at high P_{O_2}, V_{Al}''' at low P_{O_2}, with involvement of e' at medium P_{O_2}. At higher titanium concentrations the creep rate is limited by generation/recombination of defects at grain boundaries. Iron appears to increase the rate of these grain-boundary reactions. When second-phase particles of Al_2TiO_5 are present, $\dot{\varepsilon}$ is decreased but ionic conductivity is increased.

1. Introduction

The transport properties and mechanical properties of solids depend on the presence of imperfections: point defects and line defects (dislocations). In α-Al_2O_3 point defects invariably result from the presence of impurities or dopants, donor impurities promoting the formation of aluminium vacancies, oxygen interstitials and quasi-free electrons, acceptors promoting the formation of aluminium interstitials, oxygen vacancies and electron holes. Conduction involves charged point defects; diffusion may involve neutral as well as charged defects. The same applies to related properties such as creep, though here dislocations may also be involved.

In polycrystalline compounds diffusional creep involves migration of all components: in Al_2O_3 transport of aluminium and oxygen atoms from grain boundaries under stress to those not under stress. This transport may occur either through the bulk of the grains, along grain boundaries, or via both. For Al_2O_3 it is generally accepted that oxygen moves along grain boundaries, probably as a neutral species, O_i^x [1]. Aluminium, on the other hand, moves through the bulk as either Al_i''' (in acceptor-dominated material) or as V_{Al}''' (in donor-dominated material). Since charged species moving alone would set up an electric field stopping the migration, electronic defects e' or $h^{\cdot}$ must also be involved [2]. The creep rate may be limited by the diffusion of one of the species, either the charged aluminium defects or the electronic defects, or it may be limited by the creation of those defects at interfaces by interfacial reactions. In the former case the creep rate will be proportional to the defect concentration; in the latter case it is independent of these concentrations (provided the agent causing the change in defect concentrations does not affect the rate of the interfacial reactions). For Al_2O_3 : Ti, defect chemistry predicts a certain dependence of defect concentrations on titanium concentration [Ti] and oxygen pressure P_{O_2}. Such a variation is found for conduction [2–4] but not for creep [2, 5, 6] indicating that the creep rate is limited by interfacial reactions [6]. There is a problem, however: interfacial reactions can only be rate-limiting when the defect concentration has reached a certain critical value. Below this value the rate should be diffusion-limited and should be concentration-dependent. In the work described below, creep is studied under conditions where the defect concentrations are varied from low to high values by varying the concentration of a donor dopant: titanium. Since even the purest Al_2O_3 available invariably either contains acceptors or picks up acceptors during processing, variation of the titanium donor content causes the material to change from acceptor to donor domination, with a change in the type of dominant defects from Al_i''', $V_O^{\cdot\cdot}$ and $h^{\cdot}$ to V_{Al}''', O_i'' and e' at or close to the equivalence point. Since such a change is expected to be clearly noticeable in conductivity, conductivity is also studied, the conductivity types (ionic or electronic) being determined with the aid of e.m.f. measurements. The acceptors present in the undoped material are almost certainly magnesium and iron. Complete certainty of the dominant acceptor type is achieved by doping the material with a relatively large concentration of iron, i.e. studying the properties of Al_2O_3 : Fe + Ti. Such a study should also show if and how iron affects the rate of the interfacial reactions.

Since properties may be affected by dopants dis-

0022–2461/87 $03.00 + .12

solved in the Al_2O_3 as well as by those present as a second phase, solubilities were also determined, using both electron microscopy and optical techniques. A detailed description of experimental techniques, results, and their analysis is given in the doctoral thesis of one of the authors [7].

2. Experimental procedure

Alumina powder of fine nine grade was obtained from Johnson Matthey Chemicals Ltd (Royston, UK). Required amounts of a solution of dopant compounds, ferric nitrate and titanium isopropoxide were added to a suspension of the Al_2O_3 powder in isopropyl alcohol in teflon cups. Addition of NH_4OH caused formation of a hydroxide gel. After thorough mixing, the mixture was dried, then calcined at 850° C to form γ-Al_2O_3. Cylindrical boules, 1.9 cm in diameter, 1 to 1.5 cm in height, were made from this powder by hot-pressing for about one hour in a graphite die at temperatures from 1450 to 1600° C in a vacuum of 100 to 200 μm Hg at stresses of about 8000 p.s.i. (55 MPa). Transformation of γ- to α-Al_2O_3 occurs at $T > 1200$° C. Samples for the measurements of creep and conduction were cut from the boules with the aid of a diamond saw and a diamond hollow-pipe drill. Creep samples were rectangular, 7 mm × 3 mm × 3 mm; those for conductivity were cylindrical, 12 mm in diameter, 1.1 to 1.7 mm in height. Grain size d was determined from photographs of samples etched with H_3PO_4 at 320° C for 1 to 5 min, using the intercept method: $d = 1.5L/NM$, where N is the number of intercepts between grain boundaries and a line of length L drawn on a picture taken at magnification M. Samples with different grain size were made by annealing in air at temperatures higher than the test temperatures for different times and temperatures. Typically, annealing at 1500° C for 10 h led to $d = 10$ to 15 μm; annealing for 24 to 40 h gave $d = 20$ to 45 μm; 7 days at 1600° C gave $d = 110$ μm.

Details of the microstructure were examined by scanning electron microscope (SEM) or on a transmission electron microscope (TEM). The samples were mechanically thinned with a diamond disc to about 50 μm, further thinning being done by gas ion milling. Carbon coating prevented charge accumulation.

A second phase in titanium rich Al_2O_3 is known to give rise to an absorption peak at about 400 nm [8]. Therefore absorption in this region was used to monitor the presence of a second phase. The absorption was measured in diffuse reflectance using light from a deuterium lamp passed through a Perkin-Elmer E1 monochromator. A chopper was used to filter extraneous noise. Creep was measured in a constant compressive stress machine with a facility to vary the atmosphere (oxygen partial pressure) and temperature as described elsewhere [9]. Electrical conductivity was measured by a three-probe method, using a volume guard to eliminate surface and gas phase conduction [2]. Conductivity type was determined from e.m.f. measurements on oxygen concentration cells in which the atmosphere at one side (I) was kept constant, that at the other side (II) being varied [2]. Ionic transference numbers $t_i = \sigma_i/\sigma$ as $f(P_{O_2})$ are found by differentiating the e.m.f. E with respect to the varying oxygen pressure:

$$(t_i)_{II} = \frac{4F}{RT}\left(\frac{\partial E}{\partial \ln P_{O_2 II}}\right)_{P_{O_2,I}=\text{constant}}$$

where F = the Faraday constant.

3. Experimental results

Investigation of the conductivity and e.m.f. of undoped samples as $f(P_{O_2}, T)$ showed the material to be acceptor-dominated, conductivity being ionic in nature at low P_{O_2} (10^{-4} Pa), electronic (by holes) at high P_{O_2} (10^5 Pa). Conductivity was measured both under equilibrium conditions (i.e. with slow temperature variation) and under conditions in which equilibrium with the atmosphere (and possibly in the sample) was not maintained (rapid cooling: "non-equilibrium"). Parameters of the conductivity under the two conditions are given in Table I. The partial conductivities are proportional to $P_{O_2}^r$ with $r = -0.07$ for σ_i, $r = 0.17$ for σ_h. Creep rate $\dot{\varepsilon}$ can in general be represented by

$$\dot{\varepsilon} = AS^n d^{-p} P_{O_2}^r \exp(Q/kT) \quad (1)$$

where A is a constant, S the applied stress, d the grain size and Q an activation energy; n, p and r are constants characterizing the creep mechanism, k is Boltzmann's constant and T the absolute temperature. Creep rates on samples with $d < 50$ μm were found to be described by Equation 1 with parameters given in the top line of Table II. These parameters with p close to 2 indicate that the creep is controlled by bulk diffusion (Nabarro–Herring creep). At grain size above 50 μm the parameters change to $n = 2.5$, $p = 0$, $Q = 7.6$ eV indicating a change to creep by a dislocation mechanism. The value $n = 2.5$ is close to the value 3 expected for a viscous dislocation glide mechanism [10] or a dislocation climb mechanism [11]–both mechanisms that are independent of grain size. The activation energy of 7.6 eV is close to the value reported for oxygen bulk diffusion, 6.6 [12], 6.7 [13] or 7.7 [14] eV. It is therefore likely that the mechanism involves dislocation climb limited by oxygen bulk diffusion.

Creep rates for samples with titanium contents from 15 to 30 000 p.p.m. by weight with grain sizes from 5 to 55 μm were measured at temperatures from 1400 to 1500° C under stresses from 10 to 40 MPa in atmospheres with P_{O_2} from 10^5 to 10^{-4} Pa.

Parameter values in the creep rate expression (Equation 1) are given in Table II. These results make it possible to construct a figure showing creep rates at $P_{O_2} = 2 \times 10^4$ and 10^{-4} Pa as a function of titanium concentration (Fig. 1).

TABLE I Parameters of the conductivity $\sigma = \sigma_0 \exp(-H/kT)$ for undoped samples of Al_2O_3

		Equilibrium		Non-equilibrium	
P_{O_2}(Pa)	σ	$\sigma_0(\Omega^{-1}\,cm^{-1})$	H(eV)	$\sigma_0(\Omega^{-1}\,cm^{-1})$	H(eV)
10^5	σ_h	250	3.2	67.4	3
10^{-4}	σ_i	3.53×10^6	4.8	1.88×10^4	4

TABLE II Parameters of the expression $\dot{\varepsilon} \propto S^n d^{-p} P_{O_2}^r \exp(-Q/kT)$ for the creep rate $\dot{\varepsilon}$ of Al_2O_3:Ti with various amounts of titanium; grain size 5 to 55 μm

Region	[Ti]		n	p	r	Q(eV)	
	(p.p.m.)	(cm^{-3})				$P_{O_2} = 2 \times 10^4$ Pa	$P_{O_2} = 10^{-4}$ Pa
I	0	0	1.18 to 1.3	1.8	−0.03 to −0.05	5 to 5.6	
	15	7.5×10^{17}	1.25	2*	−0.01	5	
	20	10^{18}	1.1	2*	−0.01		
	60	3×10^{18}	1.15	1.82	−0.013	5.7	
	70	3.5×10^{18}		2*	−0.03		
II	100	5×10^{18}	1.13	2.05	0.03	4.76	
	200	10^{19}			0.033	4.62	4.18
	350	1.75×10^{19}	1.2	1.4	0.014	5.13	
	500	2.5×10^{19}	1.3	1.5	0.02	4.5	
III	1500	7.5×10^{19}	1.22	1	0.023	4.2	3.5
	3000	1.5×10^{20}	1.13	1	0.016	5.1	4.5
IV	6000	3×10^{20}	1.47 to 1.5	1.8	0.01 0.014	5.3 to 5.7	5.1
	9000	4.5×10^{20}	1.3 to 1.5	2.1	−0.01 −0.02	5.7 to 6.3	5.3–5.4
	12000	6×10^{20}	1.48		−0.014	5.8	5.7
	17000	8.5×10^{20}	1.6 to 1.8	2.2	−0.018	6.2 to 6.4	5.9 to 6.0
	30000	1.5×10^{21}	1.6 to 1.8	2.2	−0.016	6.5 to 6.8	6.4 to 6.6

*Estimated.

Conductivity as $f(P_{O_2}, T)$ and the e.m.f. of oxygen concentration cells and the corresponding t_i values were measured for samples doped with 60 to 17000 p.p.m. Ti by weight, partial ionic and electronic conductivities being obtained from $\sigma_i = \sigma t_i$ and $\sigma_{el} = \sigma(1 - t_i)$.

Table III gives values of pre-exponentials and activation energies for conductivities measured under equilibrium and non-equilibrium conditions. Table IV gives values of oxygen pressure exponents for partial ionic and electronic conductivities measured under equilibrium conditions, and values of these exponents for conductivities by various species expected on the basis of defect chemistry for $[Ti_{Al}^{\cdot}] \simeq 3[V_{Al}'''']$ (the V_{Al}'''' model) and $[Ti_{Al}^{\cdot}] \simeq 2[O_i'']$ (the O_i'' model). The difference in sign of the experimental values of r for samples with high and low [Ti] indicates a change from acceptor domination at low to donor domination at high titanium concentrations.

Fig. 2 shows ionic conductivities for samples with different titanium content at 1500° C under $P_{O_2} = 10^5$ Pa and 10^{-4} Pa. The minimum in σ_i at about 80 p.p.m. Ti corresponds to the titanium concentration at which acceptor domination changes to donor domination. At [Ti] > 10000 p.p.m. the conductivity is abnormally high.

Fig. 3 shows diffuse reflectance spectra in the spectral range from λ = 280 to 500 nm, showing for samples with various titanium contents annealed under various conditions a peak at 400 nm characteristic of Al_2TiO_5 in samples prepared under oxidizing conditions when [Ti] $\geqslant$ 3000 p.p.m. by weight, peak height increasing with titanium content. The peak is markedly reduced by (partial) reduction. A scanning electron microscope picture (Fig. 4) of a sample with 9000 p.p.m. Ti shows the presence of second-phase particles at grain boundaries. X-ray dispersive energy analysis shows the atomic ratio Ti/Al to be 1 : 2, indicating that the second phase is Al_2TiO_5 as expected. Under reducing conditions the solubility is much higher due to the fact that, whereas incorporation of Ti^{4+} ($= Ti_{Al}^{\cdot}$) involves formation of native ionic defects, incorporation of Ti^{3+} ($= Ti_{Al}^{\times}$) does not. The solubility of the latter is limited by the reduction energy of TiO_2 to Ti_2O_3 and by the repulsive energy resulting from the fact that the ionic radius of Ti^{3+}, 7.6 to 7.8 nm, is larger than that of Al^{3+}, 5.1 to 5.7 nm [15]. Fig. 5 shows solubilities under various conditions according to the present work as compared with results by other workers. There are indications that the solubility of Ti^{4+} is larger at grain boundaries than in the bulk of the grains [18, 19].

TABLE III Parameters of the conductivity $\sigma = \sigma_0 \exp(-H/kT)$ for samples doped with various amounts of titanium.

[Ti]		$\sigma \equiv \sigma_i(P_{O_2} = 10^5$ Pa)				$\sigma \equiv \sigma_e(P_{O_2} = 10^{-4}$ Pa)			
(p.p.m.)	(cm^{-3})	Equilibrium		Non-equilibrium		Equilibrium		Non-equilibrium	
		$\sigma_0(\Omega^{-1}cm^{-1})$	H(eV)	$\sigma_0(\Omega^{-1}cm^{-1})$	H(eV)	$\sigma_0(\Omega^{-1}cm^{-1})$	H(eV)	$\sigma_0(\Omega^{-1}cm^{-1})$	H(eV)
100	5×10^{18}	4.5×10^4	4.16	43×10^3	3.8	120	3.3	34	3.12
350	1.75×10^{19}	1.2×10^4	3.76	4.3×10^3	3.6	150	3.2	150	3.2
500	2.5×10^{19}	3.2×10^5	4.5	8.7×10^4	3.8	4×10^3	3.6	483	3.4
3000	1.5×10^{20}	472	3.0	8.2	2.55	4.2×10^5*	4.3*	3.4×10^4*	3.9*
						1.5×10^{-4}†	1.1†	2×10^{-4}†	3.9†

*$T > 1450°$ C.
†$T < 1400°$ C.

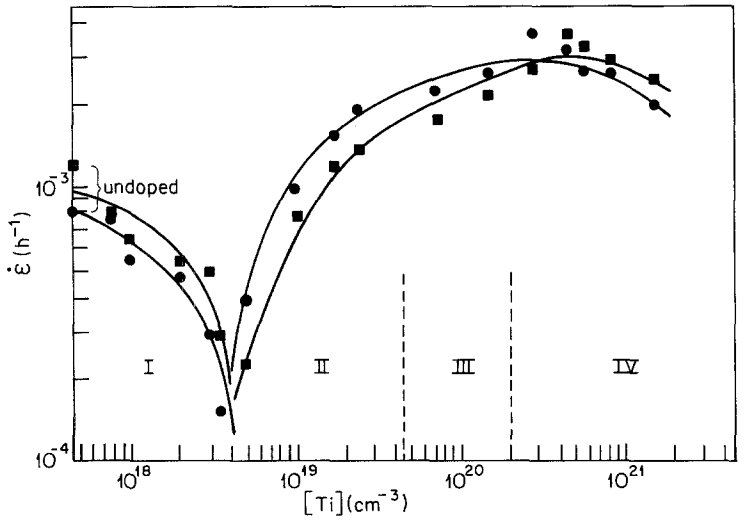

Figure 1 Creep rates as a function of titanium concentration at $T = 1450°C$, $d = 20\,\mu m$ and $S = 30\,MPa$ for P_{O_2} = (●) 2×10^4 and (■) 10^{-4} Pa.

Creep measurements similar to those described above were also performed for a series of samples with 500 p.p.m. Fe ($= 2.15 \times 10^{19}\,cm^{-3}$) and amounts of titanium varying from 200 to 7000 p.p.m. by weight (10^9 to $3.5 \times 10^{20}\,cm^{-3}$), with grain sizes from 10 to 32 μm. Table V shows values of the characteristic parameters of Equation 1. The oxygen pressure exponent r changes from negative when [Fe] > [Ti] to positive when [Ti] > [Fe] indicating again a change from acceptor domination to donor domination.

Fig. 6 shows the creep rate of the co-doped samples in air at 1450° C together with the creep rates for samples doped only with titanium as a function of the total [Ti] and (for the donor-dominated sample) as a function of the net donor concentration: [Ti] − [acceptors].

4. Discussion

The parameters for the creep rate of undoped but acceptor-dominated Al_2O_3 given in the top line of Table II indicate that the creep is bulk-diffusion controlled. The stress exponent value $n > 1$ indicates a contribution by non-viscous creep (probably grain-boundary sliding [20]) on top of viscous creep requiring $n = 1$. Similar results were reported by other workers [21]. The relatively weak P_{O_2} dependence indicates that magnesium is the major acceptor. Iron should have larger values of r, -0.17 for $V_O^{\cdot\cdot}$ or -0.25 for $Al_i^{\cdot\cdot\cdot}$ in the model dominated by $V_O^{\cdot\cdot}$, or -0.125 for $V_O^{\cdot\cdot}$ and -0.188 for $Al_i^{\cdot\cdot\cdot}$ in the $Al_i^{\cdot\cdot\cdot}$ model. Also, for Al_2O_3 : Fe pure viscous creep has been reported [5, 22]. Yet the fact that hot-pressed (i.e. reduced) samples are brown indicates that some iron is present: MgO is not reduced to metal under such conditions.

Creep results for Al_2O_3 : Ti fall in four groups, I to IV. The sign of r in Table II indicates that in Region I the material remains under acceptor control, change to donor control occurring at [Ti] = 80 p.p.m. by weight $= 4 \times 10^{18}\,cm^{-3}$. Fig. 1 shows that the creep rate decreases up to that concentration, increasing again beyond that point (Region II). The creep mechanism remains unchanged throughout Region I with approximately the same parameter values. The activation energy of 5 to 5.7 eV is close to that of ionic conductivity (Table I: 4.8 eV) suggesting involvement of the same defect species. The correctness of this idea can be checked by calculating the lattice diffusion coefficient D_l of these species from both creep and conductivity. The creep rate limited by bulk diffusion of one species (Nabarro–Herring creep) is given by

$$\dot{\varepsilon} = 14\Omega D_l S/kTd^2 \qquad (2)$$

with Ω the molecular volume, $4.25 \times 10^{-23}\,cm^3$, and S the stress. Analysis of the data on this basis gives

$$(D_l)_{\dot{\varepsilon}} = 8.5 \times 10^4 \exp(-5.8\,eV/kT) \quad cm^2\,sec^{-1} \qquad (3)$$

The Nernst–Einstein relation links ionic conductivity σ_i to the diffusion coefficient $(D_l)_\sigma$:

$$(D_l)_\sigma = \sigma_i kT/Nz^2q^2 \qquad (4)$$

with $N = \Omega^{-1}$, z the charge of the conducting species (probably $Al_i^{\cdot\cdot\cdot}$ with $z = 3$) and q the electron charge. Use of the parameters of σ_i as given in Table I leads to

$$(D_l)_\sigma = 0.226 \exp(-4.15\,eV/kT) \quad cm^2\,sec^{-1} \qquad (5)$$

TABLE IV Values of r in the expression $\sigma = AP_{O_2}^r$ of the partial ionic and electronic conductivities of Al_2O_3 : Ti and values expected for the conductivities by various species in models dominated by V_{Al}''' or O_i''

[Ti]		P_{O_2}(Pa)	$r(\sigma_i)$	$r(\sigma_e)$	V_{Al}''' model			O_i'' model		
(p.p.m.)	(cm^{-3})				V_{Al}'''	O_i''	e′	V_{Al}'''	O_i''	e′
60	3×10^{18}	10^5	−0.03	+0.21						
100	5×10^{18}	10^5	+0.21	−0.12	+0.188	+0.125	−0.25	+0.25	+0.167	−0.25
350	1.75×10^{19}	10^5	+0.22	−0.12						
500	2.5×10^{19}	10^{-4}	+0.19	−0.13						
1000	5×10^{19}	10^{-4}	+0.17	−0.05						
3000	1.5×10^{20}	10^{-4}	+0.12	−0.14						

TABLE V Parameters of the expression $\dot{\varepsilon} \propto s^n d^{-p} P'_{O_2}$ exp $(-Q/kT)$ for the creep rate $\dot{\varepsilon}$ in Al_2O_3 co-doped with 500 p.p.m. $(=2.19 \times 10^{19}\,cm^{-3})$ Fe and various amounts of titanium

[Ti]		n	p	r	Q(eV)
(p.p.m.)	(cm^{-3})				
200	10^{19}	1.32	2*	−0.012	4.6
530	2.65×10^{19}	1.21	2*	+0.01	5.0
570	2.85×10^{19}	1.12	2	+0.015	4.6
1800	9×10^{19}	0.94 to 1.22	1.4	+0.014	5.1
7000	3.5×10^{20}	1.3	1.7	+0.012	5.4

Although the parameters of Equations 3 and 5 are somewhat different, absolute values calculated from those expressions are close: 5.3×10^{-13} and $1.1 \times 10^{-13}\,cm^2\,sec^{-1}$, respectively, at 1400° C. The oxygen pressure dependencies are also close: $r = -0.07$ for σ_i, -0.03 to -0.05 for $\dot{\varepsilon}$. Therefore it is likely that creep and conductivity are limited by the same species: $Al_i^{\cdots}$, oxygen diffusing rapidly along grain boundaries. However, if the oxygen diffusion involves a neutral species, O_i^x, as it is believed to do [2], the diffusion of $Al_i^{\cdots}$ should be accompanied by the counterdiffusion of $h^{\cdot}$, and the creep rate should be described by Equation 2 with [2]

$$(D_l)_{ambipolar} = \frac{3D(Al_i^{\cdots})D(h^{\cdot})[Al_i^{\cdots}][h^{\cdot}]}{9D(Al_i^{\cdots})[Al_i^{\cdots}] + D(h^{\cdot})[h^{\cdot}]} \quad (6)$$

or, using Equation 4 with $\sigma_j = z_j q N[j]\mu_j$ and $\mu_j = (z_j q/kT)D_j$,

$$(D_l)_{ambipolar} = \frac{kT}{3Nq^2}\left(\frac{\sigma_i \sigma_h}{\sigma_i + \sigma_h}\right) \quad (7)$$

This expression predicts a change of D_l from $D_l = (kT/3Nq^2)\,\sigma_i$ when $\sigma_h > \sigma_i$ to $D_l = (kT/3Nq^2)\,\sigma_h$ in the opposite case.

At low P_{O_2}, $\sigma_h \simeq 4 \times 10^{-9}\,\Omega^{-1}\,cm^{-1}$, at high P_{O_2}, $\sigma_i = 2 \times 10^{18}\,\Omega^{-1}\,cm^{-1}$, and at the point where the partial conductivities are equal. $\sigma_i = \sigma_h = 4 \times 10^{-8}\,\Omega^{-1}\,cm^{-1}$ [7]. Hence D_l (in units $kT/3Nq^2$) should vary from 4×10^{-9} via 2×10^{-8} to 2×10^{-8} and the creep rate ($\propto D_l$) thus should increase rather than decrease as observed. Similar discrepancies exist for Al_2O_3: 60 p.p.m. Ti. Apparently creep is limited by $Al_i^{\cdots}$ at all P_{O_2}, holes not being involved because either (a) oxygen diffuses rapidly along grain boundaries in charged form (contrary to previous observations [2]) or (b) migration of holes is limited by slow generation/recombination at grain boundaries. But then electroneutrality should be maintained by still another species, probably $V_O^{\cdot\cdot}$.

In general a model involving three species: $Al_i^{\cdots}$, $V_O^{\cdot\cdot}$ and $h^{\cdot}$ might be considered. Such a model, involving V_{Al}''', O_i'' and e', will be discussed for the donor-dominated samples in Region II.

In Region II the creep rate increases with [Ti] and P_{O_2}, though with an exponent r smaller than expected for limitation by one species, V_{Al}''' – a situation similar to that met for Region I. The stress exponents n are similar to those of Region I, i.e. we are dealing with Nabarro–Herring creep with some grain-boundary sliding. The decrease of the grain-size exponent $-p$ from 2 to 1.5 indicates involvement of interface kinetics when Region III is approached.

Ionic conductivity increases with P'_{O_2} with r values close to those expected for Al_2O_3 (Table IV). It is not possible, however, to decide whether V_{Al}''' or O_i'' is the major defect compensating the charge of $Ti_{Al}^{\cdot}$. The activation energies for creep, 4.5 to 5 eV, are slightly larger than those of ionic conductivity, 4 eV.

The small P_{O_2} dependence of the creep rate can have different origins. For the sample close to the transition point from acceptor to donor domination there may still be some contribution from $Al_i^{\cdots}$ (which has a P_{O_2} dependence opposite in sign to that of V_{Al}''' and thus tends to reduce r). For the samples close to the boundary of Regions II and III a contribution by interfacial kinetics may be responsible.

Just as for Region I, a model based on ambipolar diffusion of V_{Al}''' and e' required when oxygen transport

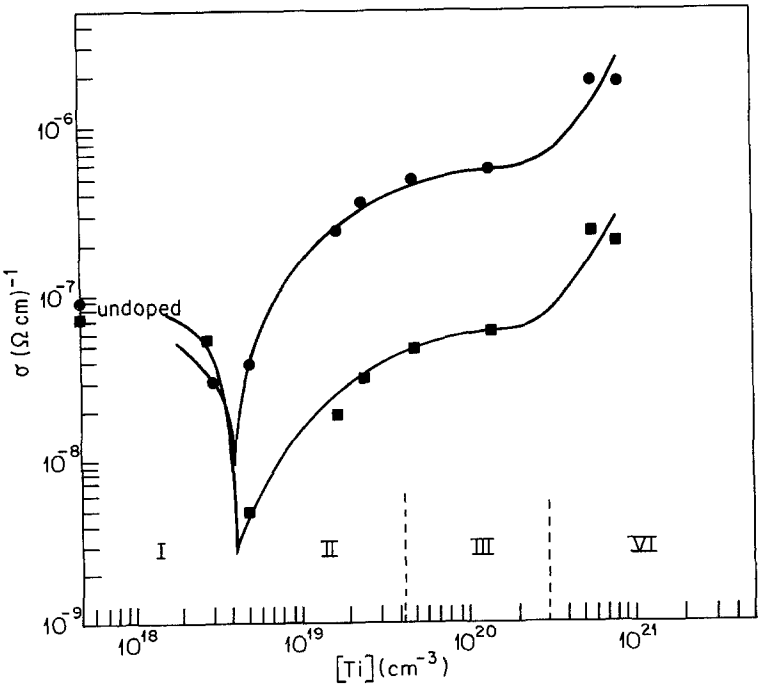

Figure 2 Partial ionic conductivites at 1500° C for samples with different titanium content at P_{O_2} = (●) 10^5 and (■) 10^{-4} Pa.

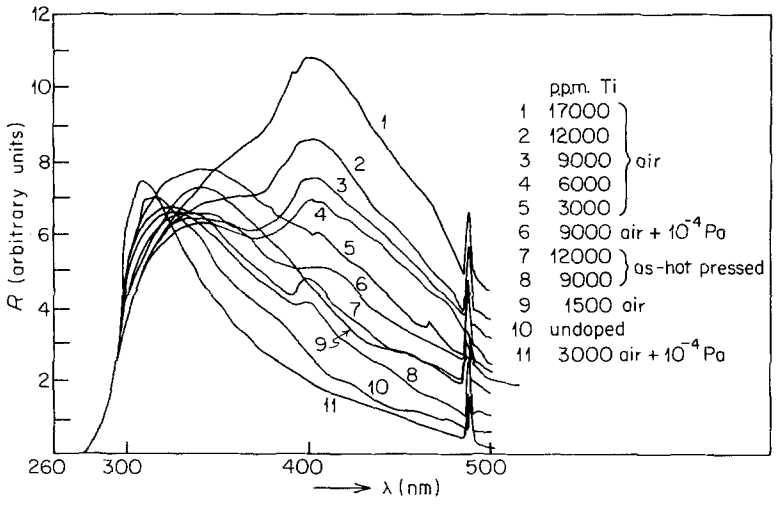

Figure 3 Diffuse reflectance of undoped Al_2O_3 and samples doped with 1500 to 17 000 p.p.m. Ti, annealed for 20 h at 1550° C under various conditions.

takes place by fast grain-boundary diffusion of O_i^x does not provide an acceptable solution. However, small r values may be accounted for by a mechanism involving bulk diffusion of three charged species: V_{Al}''', O_i'' and e′, the particle currents j satisfying

$$\sum j = 3qj(V_{Al}''') + 2qj(O_i'') + qj(e') \quad (8)$$

The general expression for $\dot{\varepsilon}$ for such a model is

$$\dot{\varepsilon} = Cj(Al_2O_3) = \frac{C}{2} j(Al)$$

$$= \frac{CD(V_{Al}''')[V_{Al}''']\{D(e)[e']\Omega_{Al} + 2D(O_i'')[O_i'']\Omega\}}{2kT\{9D(V_{Al}''')[V_{Al}'''] + 4D(O_i'')[O_i''] + D(e)[e']\}} \times \left(\frac{dS}{dx}\right) \quad (9)$$

with C a constant.

The contribution by e′ is negligible at high as well as low P_{O_2}: at high P_{O_2} because there $D(e')[e']$ is very small relative to the ionic terms, and at low P_{O_2} because $D(e')[e']$ is large leaving the ions to limit creep. In the first case Equations 8 and 9 are reduced to

$$3j(V_{Al}''') = -2j(O_i'') \quad (10)$$

and

$$\dot{\varepsilon} = \frac{CD(V_{Al}''')[V_{Al}''']D(O_i'')[O_i'']\Omega}{kT\{9D(V_{Al}''')[V_{Al}'''] + 4D(O_i'')[O_i'']\}} \left(\frac{dS}{dx}\right) \quad (11)$$

For $4D(O_i'')[O_i''] < 9D(V_{Al}''')[V_{Al}''']$ the species O_i'' will limit the creep rate, but V_{Al}''' the ionic conductivity – a difference supported by the difference in activation energies 3.76 to 4.5 eV for σ_i (Table III), 4.5 to 5.1 eV for creep (Table II). Creep rate is given by

$$\dot{\varepsilon} = \frac{C\Omega}{qkT} D(O_i'')[O_i''] \frac{dS}{dx} \quad (12)$$

For the O_i'' model dominated by $[Ti_{Al}^{\cdot}] \simeq 2[O_i'']$, preferred because of observations by Phillips *et al.* [23], we may have $4D(O_i'')[O_i''] > 9D(V_{Al}''')[V_{Al}''']$ at low P_{O_2}, and

$$\dot{\varepsilon} = \frac{C\Omega}{4kT} D(V_{Al}''')[V_{Al}'''] \frac{dS}{dx} \quad (13)$$

with V_{Al}''' limiting creep.

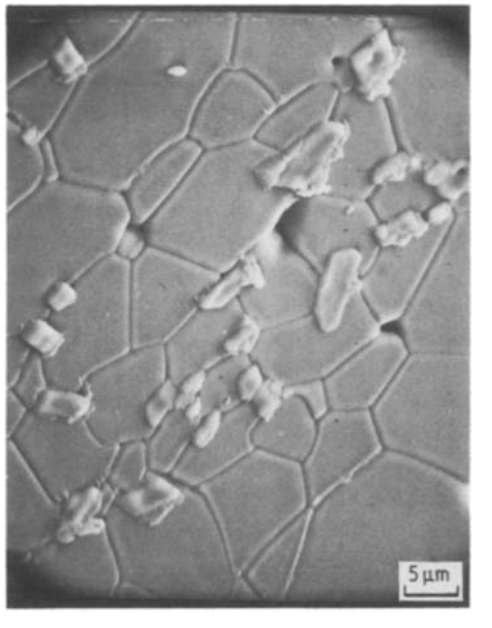

Figure 4 Scanning electron microscope picture of oxidized Al_2O_3: 9000 p.p.m. Ti.

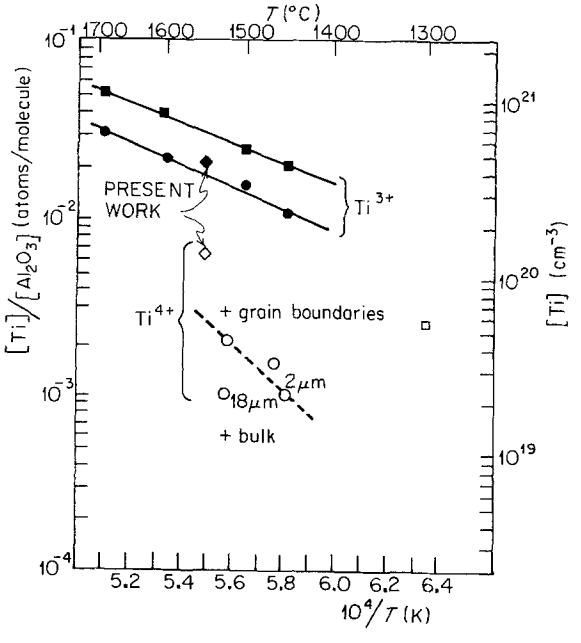

Figure 5 Solubility of titanium as $f(T)$; present results and values reported by other authors: (□) Winkler *et al.* [8], (■) McKee and Aleshin [16], (●) Roy and Coble [17], (○) Bagley *et al.* [18], (+) Kroger [19].

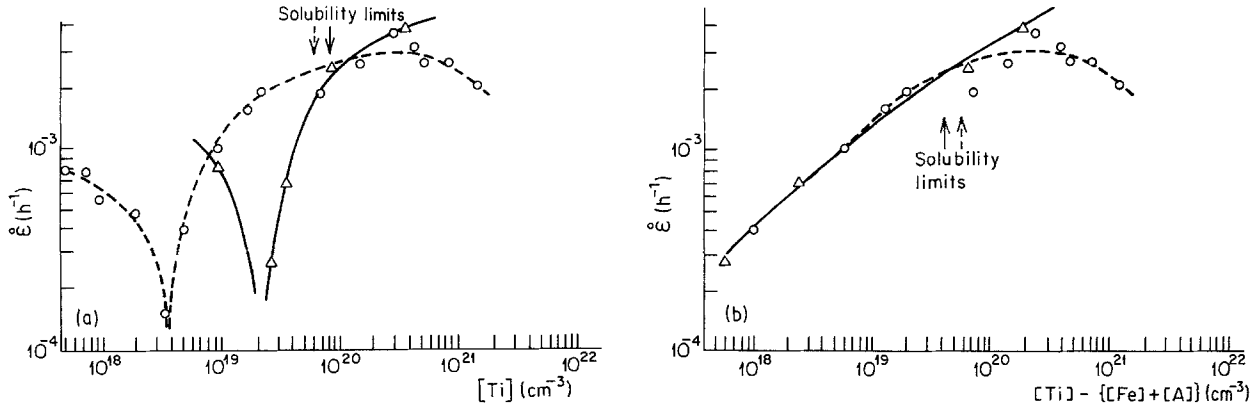

Figure 6 Creep rate as a function of titanium concentration for samples doped only with (– – –) titanium and (——) Ti + 500 p.p.m. Fe; $T = 1450°C$, $d = 20\,\mu m$, $S = 30\,MPa$ and $P_{O_2} = 2 \times 10^4\,Pa$. (*a*) Plot as $f[Ti]_{total}$; (*b*) plot as $f[Ti]_{excess}$ for the donor-dominated samples.

Only at medium P_{O_2} is e′ involved and the complete expression (Equation 9) has to be used. Using the P_{O_2} exponents of $[V_{Al}''']$, $[O_i'']$ and $[e']$ for the O_i'' model given in Table IV, at $P_{O_2} = 0.1\,Pa$ with $\sigma(V_{Al}''') \simeq \sigma(e') = 5\sigma(O_i'')$, Equation 9 leads to $\dot{\varepsilon} \propto P_{O_2}^r$ with $r \simeq 0.09$, somewhat larger than the values 0.02 to 0.33 found by us (Table II), but close to the value $r = 0.1$ reported by Hollenberg and Gordon [5].

The values of ionic conductivity at 1500° C, $P_{O_2} = 10^5\,Pa$, of the samples with 350 or 500 p.p.m. Ti, 2.5×10^{-7} and $3.5 \times 10^{-7}\,\Omega^{-1}\,cm^{-1}$ are close to those reported for single-crystalline Al_2O_3 : 430 p.p.m. Ti [4] indicating that ionic conductivity is independent of grain size at least for $d \geqslant 10\,\mu m$, a conclusion arrived at earlier by El-Aiat *et al.* [2]. The activation energies for σ_i and σ_e under equilibrium and non-equilibrium conditions are also similar to those previously reported [4] and may be interpreted in the same manner [1].

In Region III the creep rate is almost independent of [Ti]. The grain-size exponent $-p = 1$ (as also found by Ikuma and Gordon [6]): interface kinetics dominate the rate. Yet the P_{O_2} exponent $r \simeq 0.02$ and not zero as it should be for a process independent of defect concentration. However, r is much smaller than the values $r = 0.17$ and 0.12 found for σ_i (Table IV). The activation energy of creep remains unchanged (4 to 5 eV); that of σ_i has decreased to 3 eV (Table II).

If the creep rate limited by diffusion is $\dot{\varepsilon}_{NH}$ and that by interface kinetics $\dot{\varepsilon}_{IR}$, the rate limited by a combination of the two is found from $(\dot{\varepsilon})^{-1} = \dot{\varepsilon}_{NH}^{-1} + \dot{\varepsilon}_{IR}^{-1}$ which for ε_{NH} as given by Equation 2 and

$$\dot{\varepsilon}_{IR} = \frac{K_{IR}\Omega S}{kTd} \tag{14}$$

gives [6]

$$\dot{\varepsilon} = \frac{44S}{kTd^2}\left(\frac{44}{\Omega d K_{IR}} + \frac{\pi}{\Omega D_l}\right)^{-1} \tag{15}$$

where K_{IR} is the rate constant of the interfacial reaction and D_l a bulk diffusion coefficient of the rate-limiting species. For fast diffusion of oxygen along grain boundaries in neutral form as assumed in the discussion of Region II, ΩD_l is given by an expression corresponding to Equation 9:

$$\Omega D_l = \frac{3D(V_{Al}''')[V_{Al}''']\{D(e)[e']\Omega_{Al} + 2D(O_i'')[O_i'']\Omega\}}{9D(V_{Al}''')[V_{Al}'''] + 4D(O_i'')[O_i''] + D(e)[e']} \tag{16}$$

thus introducing a weak P_{O_2} dependence. The terms for electrons are important only at medium P_{O_2}. At high P_{O_2}, O_i'' limits the creep rate and V_{Al}''' the ionic conductivity. Let us now see whether $\dot{\varepsilon}$ at high P_{O_2} can be accounted for on the basis of Equation 15, assuming O_i'' to be the major native ionic defects.

The concentrations of V_{Al}''' and O_i'' are related through

$$3O_i'' = 3O_O^x + 2V_{Al}''' \tag{17}$$

with an equilibrium constant

$$K_{OV} = \frac{[V_{Al}''']^2}{[O_i'']^3}$$

Elimination of $[V_{Al}''']$ with $\sigma_i = 3q[V_{Al}''']\mu(V_{Al}''')$ gives

$$[O_i''] = K_{OV}^{-1/3}\{3q\mu(V_{Al}''')\}^{-2/3}\sigma_i^{2/3} \equiv K_O\sigma_i^{2/3} \tag{18}$$

where k_O is a new constant equal to the multiplier of $\sigma_i^{2/3}$ in the central part of Equation 18. With O_i'' the major native defect, $[O_i''] = \frac{1}{2}([Ti_{Al}^{\cdot}] - [A'])$, A′ being the acceptors present in the undoped material with $[A'] \simeq 4 \times 10^{18}\,cm^{-3}$. At high P_{O_2} $[Ti_{Al}^{\cdot}] = [Ti]_{total}$ [4]. Then for the sample with 500 p.p.m. Ti, $[O_i''] = 1.05 \times 10^{19}\,cm^{-3} = 4.49 \times 10^{-4}$ atoms per molecule of Al_2O_3. With $\sigma_i = 1.3 \times 10^{-7}\,\Omega^{-1}$ as found for the 500 p.p.m. sample, Equation 18 gives $K_O = 17.36\,(\Omega\,cm)^{2/3}$. Combining Equations 2, 17 and 18 with $D_l = D_O[O_i'']$ gives

$$\dot{\varepsilon}_{NH} = \frac{14\Omega S}{kTd^2} D_O K_O \sigma_i^{2/3} \tag{19}$$

Table VI shows experimental values of σ_i and $\dot{\varepsilon}$ ($= \dot{\varepsilon}_{exp}$) for samples with various titanium contents with $d = 20\,\mu m$ for $T = 1450°C$ and $S = 30\,MPa$, and values of $\dot{\varepsilon}_{NH}$ and $\dot{\varepsilon}$ calculated from Equations 19 and 15 using the value of K_O arrived at above, with a value of $D_O = 3 \times 10^{-8}\,cm^2\,sec^{-1}$, chosen to make $\dot{\varepsilon}_{NH} > \dot{\varepsilon}_{exp}$ at the highest titanium concentrations, and $K_{IR} = 2.73 \times 10^{-8}\,cm\,sec^{-1}$ with which Equation 14 gives $\dot{\varepsilon}_{IR} = 7.32 \times 10^{-7}\,sec^{-1}$. The agreement between $\dot{\varepsilon}$ and $\dot{\varepsilon}_{exp}$ is reasonable; only in the sample closest to the neutralization point is there a marked discrepancy.

Attempts to remove this discrepancy by basing the value of K_O on the low-concentration sample lead to values of $\dot{\varepsilon}_{NH} \leqslant \dot{\varepsilon}_{exp}$ at all concentrations, leaving no room for limitation by interfacial reactions in the high-concentration samples required by the observation that $p = 1$.

TABLE VI Calculation of creep rates of samples with $d = 20\,\mu m$ at 1450° C, $P_{O_2} = 2 \times 10^4$ Pa, $S = 30$ MPa from ionic conductivity and rate of interfacial reactions

[Ti] (p.p.m.)	[Ti] (cm^{-3})	σ_i ($\Omega^{-1}cm^{-1}$)	$[O_i'']$* (cm^{-3})	$\dot{\varepsilon}_{NH}$† (sec^{-1})	$\dot{\varepsilon}$‡ (sec^{-1})	$\dot{\varepsilon}_{exp}$ (sec^{-1})
100	5×10^{18}	2.2×10^{-8}	3.18×10^{18}	7×10^{-7}	3.59×10^{-7}	1.1×10^{-7}
350	1.75×10^{19}	1.15×10^{-7}	9.6×10^{18}	2.1×10^{-6}	5.46×10^{-6}	4.28×10^{-7}
500	2.5×10^{19}	1.3×10^{-7}	1.05×10^{19}	2.29×10^{-6}	5.58×10^{-7}	5.28×10^{-7}
1000	5×10^{19}	2.5×10^{-7}	1.61×10^{19}	3.54×10^{-6}	6.1×10^{-7}	6.11×10^{-7}
3000	1.5×10^{20}	2.3×10^{-7}	1.53×10^{19}	3.34×10^{-6}	6.0×10^{-7}	7.1×10^{-7}

*From Equation 18 with $K_O = 17.36\,(\Omega\,cm)^{2/3}$, fitting $2[O_i''] = [Ti_{Al}^{\cdot}] - [A'] = [Ti]_{total} - 4 \times 10^{18}\,cm^{-3}$ for the sample with 500 p.p.m. Ti.
†From Equation 19.
‡From Equation 15 with $K_{IR} = 2.73 \times 10^{-8}\,cm\,sec^{-1}$, Equation 14 giving $\dot{\varepsilon}_{IR} = 7.32 \times 10^{-7}\,sec^{-1}$.

In Region IV, where a second phase of Al_2TiO_5 is present, the creep rate decreases with increasing amounts of second phase, accompanied by an increase in n, p and Q, r becoming weakly negative (Fig. 1, Table II). Theories presented for such an effect are based on the presence of a threshold stress to be overcome if grain boundaries are to act as sinks or sources of point defects (which involves grain boundary dislocations [24–26]. Thus the interfacial kinetics of Region III are replaced by the lowering of activity of grain boundaries as sources or sinks. The expression of $\dot{\varepsilon}$ now is

$$\dot{\varepsilon} = K \frac{(S - S_0)^n}{d^p} \exp(-Q/kT) \qquad (20)$$

in which S_0 is the threshold stress and K is a constant proportional to $P_{O_2}^r$.

Apparent stress, grain size, and P_{O_2} exponents and activation energies n_A, p_A, r_A and Q_A are obtained from

$$n_A = \frac{d \ln \dot{\varepsilon}}{d \ln S} = \frac{nS}{S - S_0} \qquad (21)$$

$$p_A = \frac{d \ln \varepsilon}{d \ln d} = -n \frac{d \ln (S - S_0)}{d \ln d} + p \qquad (22)$$

and

$$Q_A = -R \frac{d \ln \dot{\varepsilon}}{d(T^{-1})} = Q - \frac{T^2}{(S - S_0)^n} \frac{dS_0}{dT} \qquad (23)$$

$$r_A = \frac{d \ln \dot{\varepsilon}}{d \ln P_{O_2}} = r + n \frac{d \ln (S - S_0)}{d \ln P_{O_2}} \qquad (24)$$

Since in the absence of a second phase $n = 1$, Equation 21 indicates that $n_A > 1$. With an average value of $S = 20$ MPa, the observed n values (1.5 to 1.8) correspond to $S_0 = 6.6$ to 8.9 MPa. As mentioned earlier, the solubility of titanium increases with decreasing grain size and thus S_0 should decrease, making $d \ln (S - S_0)/d \ln d$ in Equation 22 less than zero and thus $p_A > p$ or, with $p = 2$, $p_A > 2$. Values between 1 and 2 as observed close to the boundary of Regions III and IV must be attributed to limitation by both interface kinetics and the presence of a second phase.

According to Table II, $Q_A > Q$. Then Equation 23 indicates that $dS_0/dT < 0$, threshold stress decreasing with increasing temperature – a reasonable result.

Finally, since the solubility of titanium is smaller for Ti^{4+} than for Ti^{3+} while oxidation increases the ratio $[Ti^{4+}]/[Ti^{3+}]$, increase of P_{O_2} tends to increase the amount of second phase and therewith S_0, making $d \ln (S - S_0)/d \ln P_{O_2} < 0$ and $r_A < r$. Contrary to the decrease observed for creep when a second phase is present, the conductivity increases markedly (Fig. 2). Similar effects have been observed for CuCl + Al_2O_3 [27] and AgI + Al_2O_3 [28].

Results for Al_2O_3: 500 p.p.m. Fe + Ti (Table V, Fig. 6) again show a sharp minimum in the creep rate at the point where acceptor domination changes to donor domination at $[Ti] \simeq 2 \times 10^{19}\,cm^{-3}$, close to $[Fe] + [A] \simeq 2.6 \times 10^{19}\,cm^{-3}$. In the acceptor-dominated sample the creep rate is larger than in the samples without iron. At such large iron concentrations most of the iron is present as clusters, probably $(Fe_{Al}Al_iFe_{Al})^{\cdot}$ [29, 30]. This gives rise to a concentration of $Al_i^{\cdot\cdot\cdot}$ and/or $V_O^{\cdot\cdot}$, limiting creep lower than the one expected for $[Fe_{Al}^{\cdot}] \simeq 3[Al_i^{\cdot\cdot\cdot}]$ or $2[V_O^{\cdot\cdot}]$ but still larger than that expected in the absence of iron. In the donor-dominated range, $\dot{\varepsilon}$ increases with [Ti], $p = 2$, $n > 1$ and a relatively weak positive P_{O_2} dependence indicates a mechanism similar to that proposed for the singly doped samples. A plot as $f([Ti]_{excess})$ with $[Ti]_{excess} = [Ti] - [Fe] - [A]$ (Fig. 6b) shows identical behaviour for the doubly and singly doped samples.

A lowering of the p parameter from 2 to 1.4 and 1.7 in the samples with about $10^{20}\,cm^{-3}$ Ti indicates the involvement of grain-boundary kinetics. Yet, the data for the co-doped samples do not show a saturation of $\dot{\varepsilon}$. Apparently iron tends to increase K_{IR}, thus raising the level to which $\dot{\varepsilon}$ can rise before complete limitation by interfacial kinetics occurs.

The solubility limits for titanium in the two cases differ because of different acceptor content. Solubility, as determined by

$$2Al_2TiO_5 \rightarrow 2Al_2O_3 + 2Ti_{Al}^{\cdot} + 3O_O^x + O_i'' \qquad (25)$$

gives

$$[O_i''][Ti_{Al}^{\cdot}]^2 = K_{sol} a_{TiO_2}^2 \qquad (26)$$

For an estimated solubility of about $6 \times 10^{19}\,cm^{-3}$ in the single doped material at 1450° C, and $2[O_i''] = [Ti_{Al}^{\cdot}] - [A']$, $K_{sol} a_{TiO_2}^2 \simeq 1 \times 10^{59}\,cm^{-9}$. Then $2[O_i''] = [Ti_{Al}^{\cdot}] - [Fe] - [A]$ gives $[Ti] = 6.9 \times 10^{19}\,cm^{-3}$.

The titanium concentrations used in the present work are not high enough to reveal second-phase effects.

5. Summary

Creep rate and conductivity were measred for hot-pressed polycrystalline α-Al_2O_3 doped with titanium or (Fe + Ti). Both types of sample show a change from acceptor to donor domination at the point where [Ti] ≃ [acceptors]. Parameters in the creep rate expression $\dot{\varepsilon} \propto S^n d^{-p} P_{O_2}^r \exp(-Q/kT)$ indicate that bulk diffusion limits the creep rate in samples with relatively low concentrations of acceptors and titanium for grain sizes less than 50 μm. At larger grain sizes creep is limited by dislocation climb. In donor-dominated samples, the species limiting creep are O_i'' at high P_{O_2}, V_{Al}''' at low P_{O_2}, with involvement of e′ at medium P_{O_2}. Ionic conductivity always involves V_{Al}'''.

At larger [Ti], creep rate is limited by interfacial processes governing the generation/recombination of the rate-limiting defects. Iron appears to increase the rate of these processes.

Acknowledgement

This work was supported by the United States Department of Energy under Contract No. AS03-76SF001113, Project Agreement AT03-76-Er71027.

References

1. F. A. KROGER, *Adv. Ceram.* **10** (1984) 100.
2. M. M. EL-AIAT, L. D. HOU, S. K. TIKU, H. A. WANG and F. A. KROGER, *J. Amer. Ceram. Soc.* **64** (1981) 174.
3. F. A. KROGER, *Adv. Ceram.* **10** (1984) 1.
4. S. K. MOHAPATRA and F. A. KROGER, *J. Amer. Ceram. Soc.* **60** (1977) 381.
5. G. W. HOLLENBERG and R. S. GORDON, *ibid.* **56** (1973) 140.
6. Y. IKUMA and R. S. GORDON, *ibid.* **66** (1983) 139.
7. J. M. TSAUR, thesis, University of Southern California, (1985).
8. E. R. WINKLER, J. E. ARVER and I. B. CUTLER, *J. Amer. Ceram. Soc.* **49** (1966) 634.
9. L. D. HOU, S. K. TIKU, H. A. WANG and F. A. KROGER, *J. Mater. Sci.* **14** (1979) 1877.
10. J. WEERTMAN, *J. Appl. Phys.* **29** (1957) 1185.
11. F. R. N. NABARRO, *Phil. Mag.* **16** (1967) 231.
12. Y. OISHI and W. D. KINGERY, *J. Chem. Phys.* **33** (1960) 480.
13. Y. OISHI, K. ANDO and Y. KUBOTA, *ibid.* **73** (1980) 1410.
14. D. J. REED and B. J. WUENSCH, *J. Amer Ceram. Soc.* **63** (1980) 88.
15. "Handbook of Chemistry and Physics", (CRC Press, Florida, 1980/81) 16; "Handbook of Chemistry", edited by N. A. Lange (Handbook Publishers Inc, Ohio, 1944) 93; "Data on Chemicals for Ceramic Use", Bull. Nat. Research Council **118** (1949) 193.
16. W. D. MCKEE JR and E. ALESHIN, *J. Amer. Ceram. Soc.* **46** (1963) 54.
17. S. K. ROY and R. L. COBLE, *ibid.* **51** (1968) 1.
18. R. D. BAGLEY, I. B. CUTLER and D. L. JOHNSON, *ibid.* **53** (1970) 136.
19. F. A. KROGER, *ibid.* **58** (1975) 355.
20. W. R. CANNON and O. D. SHERBY, *ibid.* **60** (1977) 44.
21. R. M. CANNON and R. L. CANNON, in "Deformation of Ceramic Materials" edited by R. C. Bradt and R. E. Tressler (Plenum Press, New York, 1975) p. 61.
22. P. A. LESSING and R. S. GORDON, *J. Mater. Sci.* **12** (1977) 2291.
23. D. S. PHILLIPS, T. E. MITCHELL and A. H. HEUER, *Phil. Mag.* **42A** (1980) 417.
24. M. F. ASHBY, *Scripta Metall.* **3** (1969) 837.
25. B. BURTON, *Mater. Sci. Eng.* **11** (1973) 337.
26. J. E. HARRIS, *Metals Sci. J.* **7** (1973) 1.
27. J. B. WAGNER Jr, *Mater Res. Bull.* **15** (1980) 1691.
28. K. SHABRI and J. B. WAGNER Jr, *J. Electrochem. Soc.* **128** (1981) 6.
29. C. R. KORIPELLA, Ph.D. thesis, University of Southern California (1985).
30. C. R. KORIPELLA and F. A. KROGER, *J. Phys. Chem. Solids* in press.

Received 15 May
and accepted 23 July 1986